Disorder and interchain interactions in Peierls systems

Figge, Marc Thilo Günter

4 On the Anisotropic Random-Field Ising Model

In this chapter we present analytical results for the strongly anisotropic random-field Ising model. One of the problems to which this model has direct relevance is the lattice dimerization in disordered quasi-one-dimensional Peierls materials, such as the conjugated polymer trans-polyacetylene which we considered in Chapter 3. The model consists of weakly interacting spin chains and we combine the mean-field treatment of interchain interactions with an analytical calculation of the average chain free energy ("chain mean-field" approach). The free energy is found using a mapping on a Brownian motion model. We calculate the order parameter and give expressions for the critical random magnetic field strength below which the ground state exhibits long-range order and for the critical temperature as a function of the random magnetic field strength. The results obtained here will be used in Chapter 5 to study the experimental signature of the soliton-antisoliton confinement in quasi-one-dimensional trans-polyacetylene.

 *A first reading of this chapter should include the first two sections (4.1, 4.2) and the last two (4.5, 4.6).*

 *The main results of this chapter appeared in Physical Review B* **58**, *2626 (1998).*

4.1 Introduction

Owing to the wide range of physical systems that can be described by Ising-like models, it is believed that the random-field Ising model (RFIM), *i.e.*, the Ising model with a spatially random magnetic field, captures the essential physics of many disordered systems. Therefore, over the past two decades this model has been extensively studied, both theoretically [1] and experimentally [2]. The most studied realization of the RFIM is the dilute antiferromagnet in a uniform field. This realization was first found by Fishman and Aharony [3] in 1979 and is still under current investigation [4, 5]. Other equally interesting as diverse problems to which the RFIM has been found to be applicable are, *e.g.*, the Anderson-Mott transition of disordered interacting electrons [6], aspects of protein folding [7], and the theory of chiral order in random copolymers [8].

Much of the theoretical interest in the RFIM has originated from the early work by Imry and Ma [9]. In 1975, these authors noticed that in the presence of a random magnetic field the lowest energy state of the Ising model may have no long-range order (LRO). They considered the energetics of creating a "wrong" domain (*i.e.*, a domain in which all spins have reversed signs) of linear size R in the ordered phase. The typical domain size R caused by the disorder fluctuations is determined by the balance between the energy cost of domain walls and the possible energy gain due to the decrease of the interaction energy between the reversed spins

and the random field. In the one-dimensional case, this balance reads:

$$2I \sim 2\sqrt{\langle h^2 \rangle R}, \tag{4.1}$$

where I is the energy of one domain wall and $\langle h^2 \rangle$ is the strength of the random magnetic field. This zero temperature estimate implies that in the one-dimensional random-field Ising model LRO does not exist, as in an infinite system it is always possible to choose R large enough to make the creation of a "wrong" domain favorable. From Eq. (4.1), the zero temperature density of spin-flips is estimated to be [9, 10]:

$$n_s = \frac{1}{R} \sim \frac{\langle h^2 \rangle}{I^2}. \tag{4.2}$$

The lower critical dimension above which LRO in the RFIM is possible is 2 [9, 11].

In most previous studies of the RFIM, the interactions between the Ising spins were assumed to be isotropic, *i.e.*, independent of the direction. These studies focused on the universal critical properties of the model, such as the critical exponents and the lower critical dimension, which do not depend on the degree of anisotropy of the interactions. On the other hand, the anisotropic RFIM has several nonuniversal properties, such as the critical temperature, that are very interesting in relation to disordered quasi-one-dimensional systems.

For example, we showed in Chapter 3 that disordered Peierls chains with a doubly degenerate ground state can under certain conditions be described by the one-dimensional RFIM. In this mapping, the Ising variables describe the local lattice dimerization, while the random-field corresponds to disorder in the electron hopping amplitudes. The spin-flips induced by the random-field then correspond to disorder-induced neutral solitons in Peierls chains. The density of spin-flips is related to the magnetic properties of the disordered Peierls systems, since the neutral solitons have spin $1/2$ [12]. The conjugated polymer *trans*-polyacetylene is a well-known example of a Peierls system for which this mapping may be used. Taking into account the weak interchain interactions in quasi-one-dimensional crystalline *trans*-polyacetylene, the thermodynamics of solitons in this material may be described by the anisotropic RFIM (see Chapter 5). In this context, the interesting properties of the anisotropic RFIM are the temperature of the three-dimensional Peierls transition, the order parameter, and the density of spin-flips as a function of the random-field strength and (or) temperature. These properties strongly depend on the degree of anisotropy of the interactions.

In the present chapter we study the d-dimensional anisotropic RFIM ($d > 2$), which consists of regularly arranged chains of spins in a random magnetic field (Section 4.2). The interaction between spins in neighboring chains is supposed to be much smaller than the interaction within chains and will be treated in the mean-field approximation; the intrachain interactions will be treated exactly. Using the transfer matrix formalism and a mapping on a Brownian motion model, we find an analytical expression for the average free energy of the continuum version of our model (Section 4.3). This key result is used in Section 4.4 to obtain the order parameter, the critical temperature, and the density of spin-flips. In Section 4.4.1, we present analytical results for these quantities in the limit where thermal creation of spin-flips dominates their creation by the random magnetic field; in Section 4.4.2 we consider the opposite limit. We find the critical random-field strength below which the ground state exhibits LRO; well below the critical strength, the density of spin-flips is found to be exponentially suppressed.

In the absence of the interchain interactions, the anisotropic model reduces to the one-dimensional RFIM. In this limiting case, our solution is exact. It shows that the estimate for the density of spin-flips Eq. (4.2) in a single chain is correct to lowest order in the random magnetic field strength and gives higher-order corrections to this expression. Previous attempts to obtain an exact solution for the one-dimensional case [13] did not yield closed expressions for the free energy and the spin-flip density.

We conclude this chapter by giving the physical interpretation of our results in Section 4.5 and by summarizing in Section 4.6.

4.2 The model

We consider the anisotropic RFIM on a d-dimensional lattice with a total number of N^d sites. The Ising spins occupying the lattice, interact with their nearest neighbors and with a magnetic field that has a random value at each lattice site. The anisotropy results from the fact that the exchange interaction, I, along one of the lattice directions is assumed to be much stronger than the interaction, $I_\perp$, perpendicular to this direction: $0 < I_\perp \ll I$ (for definiteness, the interactions are chosen positive). The lattice is thus divided into N^{d-1} chains (labeled α) of N spins (labeled i). The energy of our model is given by:

$$\mathcal{E}[h] = I \sum_{\langle i,i'\rangle,\alpha} \frac{1-\sigma_{i\alpha}\,\sigma_{i'\alpha}}{2} + I_\perp \sum_{i,\langle\alpha,\alpha'\rangle} \frac{1-\sigma_{i\alpha}\,\sigma_{i\alpha'}}{2} - \sum_{i,\alpha} h_{i\alpha}\,\sigma_{i\alpha}\,. \tag{4.3}$$

Here, $\sigma_{i\alpha} = \pm 1$ is the classical spin variable describing the two possible spin directions, up and down, at site i of chain α. The summations over $\langle i,i'\rangle$ and $\langle\alpha,\alpha'\rangle$ are restricted to nearest neighbor pairs. The random magnetic field $h_{i\alpha}$ is assumed to be uncorrelated for different lattice sites, with vanishing mean and Gaussian correlator of strength ϵ:

$$\langle h_{i\alpha}\rangle = 0 \quad \text{and} \quad \langle h_{i\alpha}\,h_{j\beta}\rangle = \epsilon\,\delta_{i,j}\,\delta_{\alpha,\beta}\,. \tag{4.4}$$

Here, $\langle\ldots\rangle$ denotes the average over the random-field realizations. Finally, we impose open boundary conditions on the model. This choice does not affect our results, as these will be derived for a large system, $N \to \infty$.

For vanishing magnetic field strength ϵ, the ground state of the spin system Eq. (4.3) is ferromagnetically ordered. This is not necessarily the case when a finite random field is present: For a number of spins it may then be favorable to flip and align with the local direction of $h_{i\alpha}$ to minimize the total energy.

To calculate the partition function of the model we treat the interchain interactions in the mean-field approximation. Then the energy Eq. (4.3) becomes a sum of single-chain energies and can be written as

$$\mathcal{E}_{MF}[h] = N^{d-1} \sum_i \left[\frac{I}{2}\,(1-\sigma_i\sigma_{i+1}) - (B+h_i)\sigma_i + \frac{B^2}{\tilde{I}_\perp} + \frac{\tilde{I}_\perp}{4} \right], \tag{4.5}$$

where B is the homogeneous mean field, $\tilde{I}_\perp$ equals $I_\perp$ times the number of nearest-neighbour chains of one particular chain, and we took into account that the contributions of all N^{d-1}

chains are on average equal. The mean field B satisfies the self-consistency equation:

$$B = \frac{1}{2}\tilde{I}_{\perp}\langle\langle\sigma\rangle\rangle, \tag{4.6}$$

where $\langle\langle\ldots\rangle\rangle$ denotes both the thermal average and the average over random-field realizations. The order parameter $\langle\langle\sigma\rangle\rangle$, which is the normalized difference between the average number of sites with spin up ($N_{\uparrow}$) and spin down ($N_{\downarrow}$),

$$\langle\langle\sigma\rangle\rangle = \frac{N_{\uparrow} - N_{\downarrow}}{N_{\uparrow} + N_{\downarrow}}, \tag{4.7}$$

can be found from

$$\langle\langle\sigma\rangle\rangle = -\frac{1}{N}\frac{\partial}{\partial B}\langle F\rangle. \tag{4.8}$$

Here, $\langle F\rangle$ denotes the average over the random-field realization of the free energy of a single chain in the mean field B. For a particular random-field realization:

$$F[h] = -\frac{1}{\beta}\ln\left(\sum_{\{\sigma\}} e^{-\beta E[\sigma,h]}\right), \tag{4.9}$$

where the chain energy $E[\sigma, h]$ is given by the relevant part of Eq. (4.5),

$$E[\sigma,h] = \sum_{i}\left[\frac{I}{2}(1-\sigma_i\sigma_{i+1}) - (B+h_i)\sigma_i\right]. \tag{4.10}$$

Using Eq. (4.8), the explicit form of the self-consistency condition (4.6) becomes:

$$B = -\frac{\tilde{I}_{\perp}}{2N}\frac{\partial}{\partial B}\langle F\rangle. \tag{4.11}$$

In view of the relative weakness of the interchain interactions ($I_{\perp} \ll I$), this so-called chain mean-field approximation[14] is expected to be accurate.

The disorder-averaged free energy, $\langle F\rangle$, which we calculate analytically in the next section, can also be used to find other relevant thermodynamic properties. In particular, the average density of spin-flips inside a chain as a function of temperature and random-field strength is obtained through:

$$n_s = \frac{1}{N}\frac{\partial}{\partial I}\langle F\rangle, \tag{4.12}$$

since I is the spin-flip creation energy. In the context of the degenerate ground state conjugated polymers, mentioned in the Introduction, n_s directly gives the density of solitons within chains.

4.3 The average free energy

To derive the continuum version of the discrete model Eq. (4.10), we follow the standard path [15, 16] by first rewriting the chain partition function in the transfer matrix formalism. The

partition function is thus considered as the expectation value of an ordered product of operators $\hat{T}_i$ along the chain axis:

$$Z[h] \;=\; \sum_{\{\sigma\}} \exp\{-\beta E[\sigma,h]\} \;=\; \sum_{\sigma,\sigma'=\pm 1} \langle \sigma' | \prod_{i=1}^{N} \hat{T}_i | \sigma \rangle. \tag{4.13}$$

Here, the final summation over σ, σ' accounts for all possible boundary conditions for the spins on the chain's ends. On the basis spanned by the two vectors $|+\rangle$ and $|-\rangle$ (corresponding to $\sigma = +1$ and $\sigma = -1$, respectively), the transfer matrix $\hat{T}_i$ reads:

$$\hat{T}_i \;=\; \begin{pmatrix} e^{+\beta(h_i+B)} & e^{-\beta I}\, e^{+\beta(h_i+B)} \\ e^{-\beta I}\, e^{-\beta(h_i+B)} & e^{-\beta(h_i+B)} \end{pmatrix} . \tag{4.14}$$

$\hat{T}_i$ depends on the site-index i through the random magnetic field.

A relation between the transfer matrix Eq. (4.14) and its (euclidean) quantum Hamiltonian is established by interpreting the axis of the chain as the (imaginary) time axis of quantum mechanics. This means that neighboring sites labeled by i are considered as subsequent times t in the continuum model. In this sense $\hat{T}_i$ carries information about the time evolution of the system and can in fact be identified with the time evolution operator $\hat{T}$ of a corresponding Hamiltonian $\hat{H}$:

$$\hat{T} \;=\; \exp\{-\hat{H}\}\,. \tag{4.15}$$

In the continuum approximation the deviation of $\hat{T}$ from the identity matrix is assumed to be small, so that the last expression can approximately be written as

$$\hat{T} \;=\; 1 - \hat{H}, \tag{4.16}$$

where $\hat{H}$, obtained from Eq. (4.14), has the form:

$$\hat{H}(t) \;=\; \beta\,(h(t) + B)\,\hat{\sigma}_3 \;+\; \exp\{-\beta I\}\,\hat{\sigma}_1. \tag{4.17}$$

Here, $\hat{\sigma}_1$ and $\hat{\sigma}_3$ are the Pauli matrices and the random magnetic field is now Gaussian in time:

$$\langle h(t)\rangle \;=\; 0 \quad \text{and} \quad \langle h(t)\,h(t')\rangle \;=\; \epsilon\,\delta(t-t'). \tag{4.18}$$

In the last expression, we have chosen the lattice constant as the unit of length (time). The Hamiltonian Eq. (4.17) describes the relaxation of a spin $1/2$ in a magnetic field which has a constant x-component and a random and time-dependent z-component.

It can easily be seen from Eq. (4.14) that the validity of the expansion Eq. (4.16), *i.e.*, the validity of the continuum description of the discrete Ising model, requires the two conditions

$$\exp\{-\beta I\} \;\ll\; 1 \tag{4.19}$$

and

$$\beta\,(|h(t)| + |B|) \;\ll\; 1 \tag{4.20}$$

to be fulfilled simultaneously. While the first condition results in an upper limit for the temperature, $T \ll I$, the latter implies a lower temperature limit: $T \gg O\left(\max\left\{\sqrt{\epsilon}, |B|\right\}\right)$.

The continuum limit allows us to write the partition function Eq. (4.13) as a sum over matrix elements for the time-ordered propagation of a spin-1/2 particle in imaginary time:

$$Z[h] \;=\; \sum_{\sigma,\sigma'=\pm 1} \langle\, \sigma' \,|\, \hat{\mathcal{T}} \exp\left\{ \int_{t_i}^{t_f} \hat{H}(t)\, dt \right\} |\, \sigma \,\rangle. \tag{4.21}$$

Here, $\hat{\mathcal{T}}$ is the time-ordering operator and the integration over the dimensionless time-variable t has to be performed from the initial time $t_i = 0$ to the final time $t_f = N$ corresponding to the chain length.

It is now convenient to rotate the spinor basis over an angle $\pi/2$ around the σ_2-axis, which yields the transformed Hamiltonian:

$$\begin{aligned} \hat{H}'(t) \;&=\; \exp\left\{ i\frac{\pi}{4}\hat{\sigma}_2 \right\} \hat{H}(t)\, \exp\left\{ -i\frac{\pi}{4}\hat{\sigma}_2 \right\} \\ &=\; -\beta\,(h(t) \,+\, B)\,\hat{\sigma}_1 \;+\; \exp\{-\beta I\}\,\hat{\sigma}_3, \end{aligned} \tag{4.22}$$

and

$$Z[h] \;=\; 2\,\langle + |\, \hat{\mathcal{T}} \exp\left\{ \int_0^N \hat{H}'(t) dt \right\} |\, + \rangle. \tag{4.23}$$

To make this expression more compact, we introduce the wave function of the spin,

$$\Psi(t) \;=\; \psi_\uparrow(t)\,|+\rangle \;+\; \psi_\downarrow(t)\,|-\rangle\;, \tag{4.24}$$

which obeys the time-dependent Schrödinger-like equation,

$$\frac{d}{dt}\,\Psi(t) \;=\; \hat{H}'(t)\,\Psi(t)\;. \tag{4.25}$$

Together with the inital condition $\Psi(t = 0) = |+\rangle$, the partition function Eq. (4.23) now simply reads:

$$Z[h] \;=\; 2\,\psi_\uparrow(N). \tag{4.26}$$

Our problem of calculating the partition function has, of course, not been solved in going from Eq. (4.13) to Eq. (4.26). However, it is possible to find a substitution for the spin wave function Eq. (4.24) that relates the calculation of $Z[h]$ to an exactly solvable Brownian motion model. We introduce the two time-dependent functions $u(t)$ and $v(t)$, such that the spin wave function Eq. (4.24) reads:

$$\Psi(t) \;=\; u(t) \begin{pmatrix} \cosh(\frac{v(t)}{2}) \\ \\ \sinh(\frac{v(t)}{2}) \end{pmatrix}\;, \tag{4.27}$$

and the initial condition, $\Psi(t = 0) = |+\rangle$, requires that $u(t = 0) = 1$ and $v(t = 0) = 0$. From Eq. (4.25) we obtain two coupled differential equations for $u(t)$ and $v(t)$. The differential equation for $u(t)$ is given by

$$\frac{du(t)}{dt} \;=\; u(t)\, e^{-\beta I}\, \cosh(v(t))\;, \tag{4.28}$$

and can be easily integrated, yielding

$$u(t) \;=\; u(0)\,\exp\left\{\, e^{-\beta I}\int_0^t \cosh(v(t'))\,dt' \,\right\} \tag{4.29}$$

as a function of $v(t)$. The differential equation for $v(t)$, on the other hand, does not depend on $u(t)$ and is given by

$$\frac{dv(t)}{dt} \;=\; -\,2\,\beta\,B \,-\, 2\,e^{-\beta I}\,\sinh(v(t)) \,-\, 2\,\beta\,h(t)\;. \tag{4.30}$$

This equation can be interpreted as the Langevin equation for the velocity v of a particle that undergoes a one-dimensional Brownian motion. The first and the second terms in Eq. (4.30) describe, respectively, a constant (bias) force and a v-dependent friction force, while the last term is the random force acting on the particle. As an example one could think of the one-dimensional motion of a flying feather under the influence of the earth gravitation, the air friction, and the random forces of wind.

In the absence of the random force (no random magnetic field, $h(t) \equiv 0$), it is straightforward to obtain $v(t)$ from Eq. (4.30) and for $t \to \infty$ the velocity approaches a time-independent value

$$v_\infty \;=\; -\,\mathrm{arcsinh}\Big(\beta\,B\,e^{\beta I}\Big)\;. \tag{4.31}$$

In the presence of the random force, $v(t)$ becomes a stochastic variable with a time-dependent probability distribution $P(v,t)$. Integrating the Langevin equation (4.30) over a short-time intervall Δt,

$$\Delta v \;=\; -\,\big(2\,\beta\,B \,+\, 2\,e^{-\beta I}\,\sinh(v)\big)\,\Delta t \;-\; 2\,\beta\int_t^{t+\Delta t} dt' h(t') \;+\; \mathcal{O}(\Delta t^2)\;, \tag{4.32}$$

one can calculate the n'th jump moment,

$$\alpha_n(v) \;=\; \lim_{\Delta t\to 0}\frac{\langle \Delta v^n\rangle}{\Delta t}\;, \tag{4.33}$$

which is the averaged ratio of the n'th moment of the velocity change Δv for the Brownian particle with velocity $v(t)$ and the corresponding time interval Δt after time t. It follows from Eq. (4.32) that the first and second moments are given by, respectively,

$$\alpha_1(v) \;=\; -2\beta B \;-\; 2\,e^{-\beta I}\,\sinh(v)\;, \tag{4.34}$$

and

$$\alpha_2 \;=\; 4\beta^2\int_0^N \langle h(t)h(t')\rangle\,dt' \;=\; 4\,\beta^2\epsilon\;, \tag{4.35}$$

while

$$\alpha_n(v) \;=\; 0 \qquad \text{for} \quad n \geq 3\;, \tag{4.36}$$

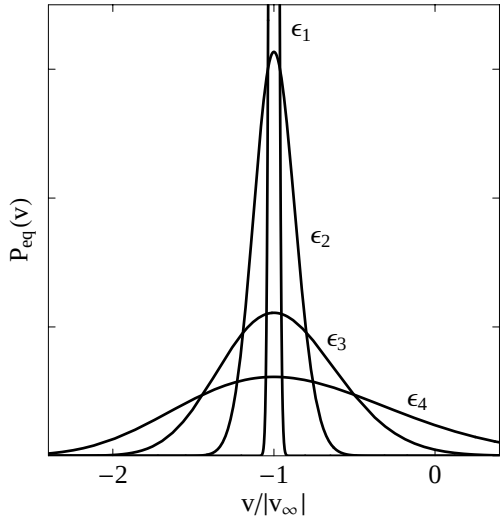

Figure 4-1: *Plot of the equilibrium distribution* $P_{eq}(v)$ *for four different values of the fluctuation strength,* $\epsilon_4 > \epsilon_3 > \epsilon_2 > \epsilon_1 \to 0$*, keeping* v_∞ *fixed.*

as $h(t)$ is Gaussian according to Eq. (4.18). The time-dependent probability distribution $P(v,t)$ is obtained from the master equation for Markovian processes [17, 18],

$$\frac{\partial P(v,t)}{\partial t} = \sum_{n=1}^{\infty} \frac{(-1)^n}{n!} \frac{\partial^n}{\partial v^n} \alpha_n(v)\, P(v,t)\,, \tag{4.37}$$

which is a '*gain–loss*'-equation for the probability as a function of the velocity v. It follows from Eq. (4.36) that the master equation (4.37) reduces to the so-called Fokker-Planck equation and in the limit of long times ($N \to \infty$) the time-independent equilibrium distribution, $P_{eq}(v)$, is reached, obeying:

$$\frac{\partial P_{eq}(v)}{\partial t} = -\frac{\partial}{\partial v}\Big(\alpha_1(v) P_{eq}(v)\Big) + \frac{\alpha_2}{2}\frac{\partial^2 P_{eq}(v)}{\partial v^2} = 0\,. \tag{4.38}$$

The solution of the Fokker-Planck equation (4.38) is easily found to be:

$$P_{eq}(v) = \mathcal{N} \exp\Big\{-\eta\, v - z\cosh(v)\Big\}, \tag{4.39}$$

where we introduced

$$\eta = \frac{B}{\beta\epsilon}\,, \tag{4.40}$$

and

$$z = \frac{e^{-\beta I}}{\beta^2 \epsilon}\,, \tag{4.41}$$

while the normalization coefficient $\mathcal{N}$ is determined from the condition $\int_{-\infty}^{+\infty} dv P_{eq}(v) = 1$. In Figure 4-1 we plot the equilibrium distribution Eq. (4.39) for several values of the fluctuation

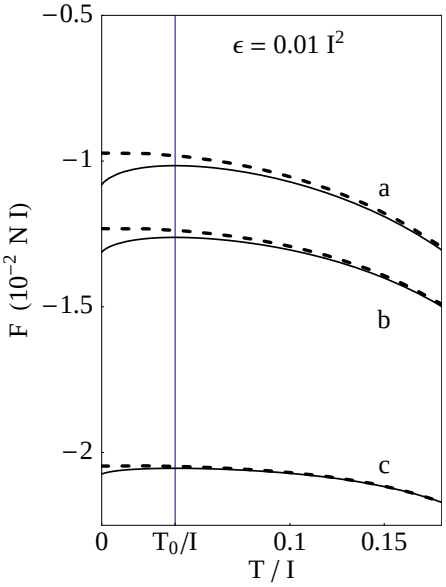

Figure 4-2: *The average free energy of the anisotropic RFIM as a function of temperature for three values of the mean field:* $B = 0.005I$, $0.01I$, *and* $0.02I$ *(curves a, b, and c, respectively). Solid curves represent the analytical result Eq. (4.43) for the continuum approximation to the RFIM; dashed curves are obtained from numerical simulations of the RFIM. In all cases, the random-field strength was taken* $\epsilon = 0.01I^2$. *The thin line at* $T = T_0$ *gives the position of the maxima of the analytical solution.*

strength ϵ keeping $\nu_\infty = -\mathrm{arcsinh}(\eta/z)$ fixed. It is seen, that $P_{eq}(\nu)$ is centered around ν_∞ with a width that depends on the strength of the fluctuations, while its asymmetry with respect to ν_∞ is due to the first term in the exponential Eq. (4.39) originating from the constant bias force ($\eta \propto B$). In the limit of vanishing fluctuations ($\epsilon \to 0$), $P_{eq}(\nu)$ approaches a δ-distribution, $P_{eq}(\nu) \to \delta(\nu - \nu_\infty)$.

Using our result for $P_{eq}(\nu)$, the average free energy of the RFIM can easily be obtained. We first note that Eq. (4.29) enables us to write the partition function Eq. (4.26) in terms of $\nu(t)$ alone:

$$\begin{aligned} Z[h] &= 2\,\psi_\uparrow(N) = 2\,u(N)\,\cosh\left(\frac{\nu(N)}{2}\right) = \\ &= 2\,\exp\left\{ e^{-\beta I}\int_0^N \cosh(\nu(t))\,dt \right\}\cosh\left(\frac{\nu(N)}{2}\right). \end{aligned} \tag{4.42}$$

Omitting in the limit of long chains all terms that do not grow proportional to N, we can now replace the average of $\ln Z[h]$ over the random-field realizations by the average over $P_{eq}(\nu)$. This leads to

$$\frac{1}{N}\,\langle F\rangle = -\frac{e^{-\beta I}}{\beta}\int_{-\infty}^{+\infty} P_{eq}(\nu)\cosh(\nu)\,d\nu = B\,\frac{z}{\eta}\,\frac{K'_\eta(z)}{K_\eta(z)}\,, \tag{4.43}$$

where $K_\eta(z)$ denotes the modified Bessel function of order η and $K'_\eta(z)$ its derivative with respect to z [19]. In the limit of vanishing interchain interactions, $\eta \propto B \to 0$, the result Eq. (4.43) corresponds to the expression Eq. (3.44) that has been used in Section 3.3 in the context of a weakly disordered Peierls chain.

The analytical solution Eq. (4.43) of the average free energy is the key result of this chapter, from which all further results follow. In Figure 4-2, this solution as a function of temperature is compared to results of a numerical simulation of the discrete RFIM at $\epsilon = 0.01\,I^2$ for three values of the mean field B. Apart from the presence of the mean field, the simulation method is identical to the one described in Section 3.5. Figure 4-2 shows that in the temperature region $T \ll I$, the analytical solution is in excellent agreement with the simulation, except for very low temperatures, where the condition Eq. (4.20) is not met. It is observed that the analytical solution for the free energy reaches a maximum at $T = T_0(\epsilon) \neq 0$ (indicated by the thin line). The meaning of $T_0(\epsilon)$ will be discussed in Section 4.4.2.

4.4 Analysis of results

Using Eq. (4.43), it is straightforward to solve numerically the self-consistency equation (4.11), from which the order parameter $\langle\langle\sigma\rangle\rangle$ is found through Eq. (4.6). Figure 4-3 gives the thus obtained order parameter as a function of temperature and random-field strength for $\tilde{I}_\perp/I = 0.02$. A low-temperature cut-off $T_0(\epsilon)$ was used, as will be explained in detail in Section 4.4.2. The thick curve in the $\langle\langle\sigma\rangle\rangle = 0$ plane separates the region with LRO (inside this curve) from the one without LRO. From the solution for $\langle\langle\sigma\rangle\rangle$, one obtains the critical temperature and the density of spin-flips through further numerical analysis. For certain parameter values η and z, however, our result Eq. (4.43) also allows for analytical solutions. Here, two limiting cases should be distinguished. In Section 4.4.1, we will consider the case of very weak disorder, where thermally induced spin-flips dominate the ones induced by the random magnetic field. In Section 4.4.2, we consider the opposite limit.

4.4.1 Dominant thermal spin-flips

For a weak random magnetic field ($\epsilon \to 0$) the modified Bessel function in Eq. (4.43) has to be evaluated at large order and argument $(\eta, z \gg 1)$. Using standard expansions [19], we obtain to first order in ϵ:

$$\frac{1}{N}\langle F\rangle \;=\; -\frac{1}{\beta}\sqrt{(\beta B)^2 + e^{-2\beta I}} \;-\; \frac{\beta\epsilon}{2}\,\frac{e^{-2\beta I}}{(\beta B)^2 + e^{-2\beta I}}\,. \tag{4.44}$$

The first term in the right hand side of Eq. (4.44) is the continuum approximation for the free energy of the discrete model Eq. (4.10) at $\epsilon = 0$, as it can be obtained directly by performing the average of the free energy Eq. (4.43) with the δ-distribution $P_{eq}(\nu) = \delta(\nu - \nu_\infty)$, where ν_∞ is given by Eq. (4.31). Under the conditions specified by Eqs. (4.19) and (4.20) this term agrees with the exact expression,

$$\frac{1}{N}F \;=\; -\frac{1}{\beta}\,\ln\left(\cosh(\beta B) + \sqrt{(\sinh(\beta B))^2 + e^{-2\beta I}}\right)\,, \tag{4.45}$$

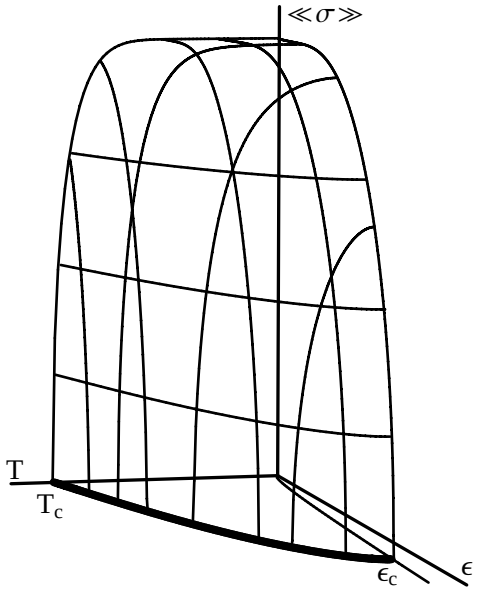

Figure 4-3: *The order parameter $\langle\langle\sigma\rangle\rangle$ of the ansitropic RFIM as a function of the random magnetic field strength ϵ and temperature T (for $T > T_0(\epsilon)$). The plot was obtained by solving the self-consistency condition Eq. (4.11) with the analytical solution Eq. (4.43) for the free energy. The interchain interaction was chosen such that $\tilde{I}_\perp/I = 0.02$, in which case $T_c \simeq 0.295I$ (at $\epsilon = 0$) and $\epsilon_c = 0.0071I^2$. At $(T,\epsilon) = (0,0)$, the order parameter reaches its maximum: $\langle\langle\sigma\rangle\rangle = 1$. The thick curve in the $\langle\langle\sigma\rangle\rangle = 0$ plane separates the (ϵ, T) regions with and without long-range order.*

which can be obtained by diagonalization of the transfer-matrix Eq. (4.14) at $h_i = 0$.

Using Eq. (4.44), the self-consistency equation (4.11) for the mean field B can be written in the form:

$$\frac{2T}{\tilde{I}_\perp} = y - \frac{\epsilon}{T^2} e^{-2\beta I} y^4 , \tag{4.46}$$

where

$$y = \left[(\beta B)^2 + e^{-2\beta I}\right]^{-\frac{1}{2}} . \tag{4.47}$$

At the transition temperature, $T_c(\epsilon)$, the order parameter vanishes. Therefore, by putting $B = 0$ in Eq. (4.46), we obtain an equation for $T_c(\epsilon)$:

$$\frac{2T_c(\epsilon)}{\tilde{I}_\perp} = \exp\left(\frac{I}{T_c(\epsilon)}\right) - \frac{\epsilon}{T_c^2(\epsilon)} \exp\left(2\,\frac{I}{T_c(\epsilon)}\right) . \tag{4.48}$$

In particular, at $\epsilon = 0$ we obtain:

$$\frac{\tilde{I}_\perp}{2T_c(0)} \exp\left(\frac{I}{T_c(0)}\right) = 1 . \tag{4.49}$$

This equation can be compared with the exact result for the critical temperature of the two-dimensional Ising model [20, 21]:

$$\sinh\left(\frac{I_\perp}{T_c}\right)\sinh\left(\frac{I}{T_c}\right) = 1. \tag{4.50}$$

For $I_\perp \ll I$, both Eq. (4.49) and Eq. (4.50) give approximately:

$$T_c \sim \frac{I}{\ln\left(\frac{I}{I_\perp}\right)}, \tag{4.51}$$

which shows that the chain mean-field approximation works well for the strongly anisotropic Ising model.

From Eq. (4.48) we find that at weak disorder the transition temperature decreases linearly with ϵ,

$$T_c(\epsilon) = T_c(0)\,(1 - \alpha\,\epsilon), \tag{4.52}$$

where α is:

$$\alpha = \frac{2}{\tilde{I}_\perp\,(I + T_c(0))}. \tag{4.53}$$

Finally, the average density of spin-flips [see Eq. (4.12)] for weak disorder is given by

$$n_s = \begin{cases} e^{-\beta I} & \text{for} \quad T > T_c(\epsilon) \\ e^{-2\beta I}\left(\frac{2}{\tilde{I}_\perp\,\beta} + \epsilon\beta^2 y^2\right) & \text{for} \quad T < T_c(\epsilon) \end{cases} \tag{4.54}$$

We note, that in the disordered phase (above $T_c(\epsilon)$), no correction to the density of spin-flips linear in ϵ occurs. This is related to the fact that in the weak disorder limit, the domain size R in Eq. (4.1) is limited by the distance between thermally induced spin-flips, which is too small to allow for the creation of spin-flips by the random field. In this case the lowest-order correction is $\epsilon^2\beta^4\exp(\beta I)/8$.

4.4.2 Dominant disorder-induced spin-flips

We now turn to the limit $\exp[-\beta I] \ll \beta^2\epsilon$, or equivalently: $z \ll 1$, where the thermal creation of spin-flips is negligible compared to creation by the random magnetic field. To lowest order in z, we then have [19] in Eq. (4.43):

$$\frac{z}{\eta}\frac{K'_\eta(z)}{K_\eta(z)} \simeq -\frac{\Gamma(1+\eta)\left(\frac{z}{2}\right)^{-\eta} + \Gamma(1-\eta)\left(\frac{z}{2}\right)^{\eta}}{\Gamma(1+\eta)\left(\frac{z}{2}\right)^{-\eta} - \Gamma(1-\eta)\left(\frac{z}{2}\right)^{\eta}}. \tag{4.55}$$

To find the critical temperature, at which $B \to 0$, it is sufficient to consider only small values of $\eta \propto B$, where $\Gamma(1 \pm \eta) \simeq e^{\mp\gamma\eta}$ ($\gamma \simeq 0.577$ is Euler's constant), so that Eq. (4.55) further reduces to:

$$\frac{z}{\eta}\frac{K'_\eta(z)}{K_\eta(z)} \simeq -\frac{1}{\tanh(\eta\,\ln\frac{2e^{-\gamma}}{z})}. \tag{4.56}$$

Using this result and the definitions Eq. (4.40) and Eq. (4.41) of η and z, respectively, the free energy Eq. (4.43) finally becomes:

$$\frac{1}{N}\langle F\rangle = -\frac{\epsilon}{I(T,\epsilon)}\frac{x}{\tanh(x)}. \tag{4.57}$$

Here, we introduced

$$I(T,\epsilon) = I - 2T\ln\left(\frac{T}{e\,T_0}\right), \tag{4.58}$$

with

$$T_0 = T_0(\epsilon) = \sqrt{2\,e^{-\gamma-2}\,\epsilon}\ , \tag{4.59}$$

a characteristic temperature that depends on the strength of the random magnetic field. Furthermore, we defined x,

$$x = \frac{I(T,\epsilon)B}{\epsilon}\ . \tag{4.60}$$

At $T = T_0$, the free energy reaches a maximum (cf. Figure 4-2), implying that the entropy vanishes. The general expression for the entropy in our model is:

$$\langle S\rangle = -\frac{1}{N}\frac{\partial\langle F\rangle}{\partial T} = \frac{2\,\epsilon}{I(T,\epsilon)^2}\frac{x^2}{\sinh^2(x)}\ln\left(\frac{T}{T_0}\right), \tag{4.61}$$

which becomes negative for $T < T_0$. This unphysical behavior is also observed for isolated chains ($I_\perp = 0$). Its origin is the continuum approximation, which breaks down at low temperatures. As we discussed in Section 3.4, the problem arises due to the fact that in the continuum model a spin-flip can take any position on the chain and is not restricted to the lattice points of the original discrete model. The continuum model, therefore, gives incorrect results as soon as the thermal fluctuation of the spin-flip positions, $l(T) \sim T^2/\epsilon$, becomes less than one lattice constant. This happens at $T < \sqrt{\epsilon}$, in agreement with Eq. (4.59). The nature of T_0 suggests that at this temperature the continuum model in fact describes the zero temperature discrete model. Using numerical simulations, we confirmed that for the one-dimensional RFIM this indeed is a reasonable identification (see Section 3.5).

Using Eq. (4.57), the self-consistency condition Eq. (4.11) now takes the form:

$$\langle\langle\sigma\rangle\rangle = \frac{2B}{\tilde{I}_\perp} = \frac{1}{\tanh(x)} - \frac{x}{\sinh^2(x)}\ . \tag{4.62}$$

For $\langle\langle\sigma\rangle\rangle \ll 1$, the non-trivial solution of Eq. (4.62) for the order parameter reads:

$$\langle\langle\sigma\rangle\rangle \propto \sqrt{I(T,\epsilon) - \frac{3\epsilon}{\tilde{I}_\perp}}\ . \tag{4.63}$$

At the critical temperature $T_c(\epsilon)$, the left hand side of Eq. (4.63) vanishes, yielding

$$\frac{\tilde{I}_\perp}{3\epsilon}\left(I - 2\,T_c(\epsilon)\ln\left(\frac{T_c}{e T_0(\epsilon)}\right)\right) = 1\ . \tag{4.64}$$

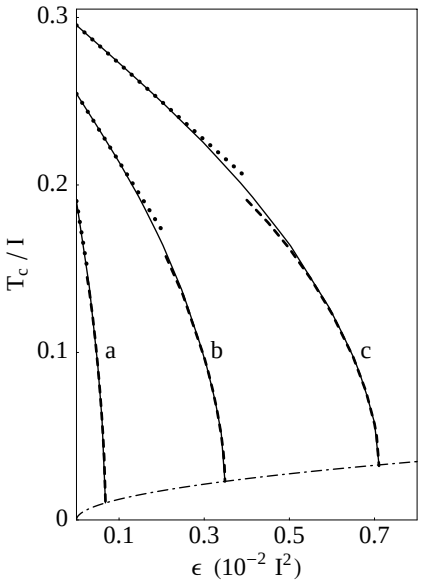

Figure 4-4: *The critical temperature* $T_c(\epsilon)$ *of the anisotropic RFIM as a function of the random magnetic field strength for* $\tilde{I}_\perp/I = 0.002$, *0.01, and 0.02 (curves a, b, and c, respectively). Solid curves derive from solving Eq. (4.11) with the exact free energy Eq. (4.43). The dashed curves are obtained by solving Eq. (4.64), while the dots represent the small-*ϵ *behaviour Eq. (4.52). The dash-dotted curve shows the temperature* $T_0(\epsilon)$, *below which the continuum approximation breaks down and which corresponds approximately to* $T = 0$ *in the discrete RFIM.*

Figure 4-4 shows the critical temperature as a function of the random magnetic field strength for three values of the interchain interaction. The dashed curves are obtained by solving Eq. (4.64). This yields meaningful results only for $T_0(\epsilon) \leq T_c(\epsilon) \leq 0.15I$, where the upper limit arises from the fact that the $z \ll 1$ approximation made in deriving Eq. (4.55) starts to break down. The solid curves show the results obtained if we do not apply the small-z expansion, but instead numerically solve the self-consistency equation Eq. (4.11) with the full free energy Eq. (4.43). Clearly, over a large disorder interval, the approximate results give excellent agreement with the exact ones. Also presented (dots) are the results in the weak disorder limit (Eq. (4.52)). The dash-dotted curve in Figure 4-4 indicates the lower temperature limit $T_0(\epsilon)$, which we argued to correspond to $T = 0$ in the discrete model. The critical disorder strength ϵ_c below which LRO exists in the ground state is a function of the interchain interaction and can be calculated from Eq. (4.64) by requiring that $T_c(\epsilon) = T_0(\epsilon)$. This yields

$$\epsilon_c \approx \frac{\tilde{I}_\perp I}{3}\left(1 + \frac{c}{9}\sqrt{\frac{3\tilde{I}_\perp}{I}}\right), \tag{4.65}$$

where

$$c = 2\sqrt{2e^{-\gamma-2}} \simeq 0.78. \tag{4.66}$$

It is seen that ϵ_c is of the order of $\tilde{I}_\perp I$. For a random-field strength $\epsilon \ll \epsilon_c$, the ground

state ($T = T_0$) of the anisotropic RFIM is nearly perfectly ordered, $\langle\langle\sigma\rangle\rangle \simeq 1$, as is clear from Figure 4-3.

We now turn to the average density of spin-flips within the chains, which using Eqs. (4.12) and (4.57), is obtained as:

$$n_s(T,\epsilon) \;=\; \frac{\epsilon}{I^2(T,\epsilon)}\,\frac{x^2}{\sinh^2(x)}\;. \tag{4.67}$$

In the disordered phase ($x = 0$), Eq. (4.67) reduces to

$$n_s(T,\epsilon) \;=\; \frac{\epsilon}{I^2(T,\epsilon)}\;. \tag{4.68}$$

In particular, the latter expression holds for the one-dimensional RFIM, which is disordered at all temperatures [9, 10]. The temperature region where Eq. (4.68) is valid is specified by Eqs. (4.19) and (4.20). However, as the numerical calulations in Section 3.5 (see Figure 3-7) show, the density of spin-flips at zero temperature in the discrete RFIM is very close to the continuum result Eq. (4.68) at $T = T_0(\epsilon)$:

$$n_s(0,\epsilon) \;\approx\; \frac{\epsilon}{\left(I + c\sqrt{\epsilon}\right)^2}\;, \tag{4.69}$$

where c is defined by Eq. (4.66). To lowest order in ϵ, this result agrees with the estimate Eq. (4.2). The leading correction to Eq. (4.2) is of the order $\epsilon^{3/2}$. For $\epsilon < \epsilon_c$, LRO does exist and the zero temperature spin-flip density should be obtained by numerically solving the order parameter from Eq. (4.62) at $T = T_0$ and substituting the result into Eq. (4.67). For $\tilde{I}_\perp/I = 0.02$ the resulting ϵ-dependence of the spin-flip density is shown in Figure 4-5. At this particular value of the interchain interaction, the critical disorder strength is $\epsilon_c \simeq 0.0071\,I^2$. It is observed from Figure 4-5 that well below this critical value, the spin-flip density is strongly suppressed. In fact, for $\epsilon \ll \epsilon_c$, Eq. (4.67) reduces to

$$n_s(T_0,\epsilon) \;\simeq\; \frac{\tilde{I}_\perp^2}{\epsilon}\,\exp\!\left(-\,\frac{\tilde{I}_\perp\, I(T_0,\epsilon)}{\epsilon}\right)\;, \tag{4.70}$$

which shows exponential suppression for small ϵ. Equation (4.70) is represented in Figure 4-5 by the dashed curve. It should be noted that, strictly speaking, Eq. (4.70) is only valid for $\eta = B/(\beta\epsilon) \ll 1$ which was assumed in deriving Eq. (4.56) from Eq. (4.55). For $\tilde{I}_\perp/I = 0.02$ and $T = T_0$, this condition on η implies $\epsilon \gg \tilde{I}_\perp^2 \sim O(10^{-4})$, which holds for the overwhelming part of Figure 4-5.

4.5 Discussion

The results for the anisotropic Ising model obtained above admit a simple interpretation. To this end it is useful to distinguish between two kinds of spin-flips occuring in chains: kinks and antikinks. For kinks, the spins are positive to the left of the spin-flip and negative to the right. For antikinks, the opposite holds. Obviously, kinks and antikinks have the same creation energy, and along the chain always an alternation of kinks and antikinks occur.

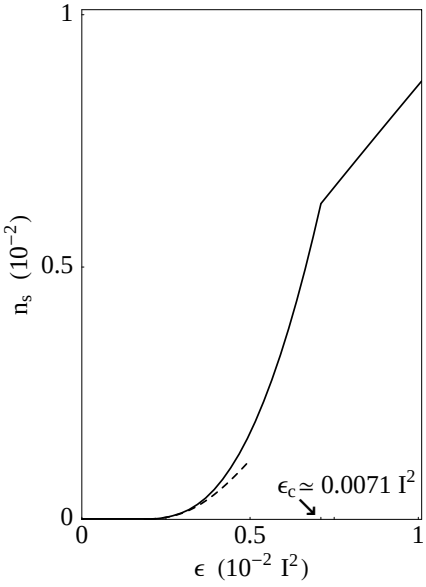

Figure 4-5: *Density of spin-flips within the chains of the ansitropic RFIM as a function of the random magnetic field strength at* $T = T_0$*, i.e., in the ground state. The interchain interaction was chosen such that* $\tilde{I}_\perp / I = 0.02$*. The dashed line shows the analytical result Eq. (4.70) for* $\epsilon \ll \epsilon_c \simeq 0.0071 I^2$.

We first discuss the density of thermally induced spin-flips in the absence of a random magnetic field (Eq. (4.54) with $\epsilon = 0$). As we assumed the temperature to be much smaller than the spin-flip creation energy, I, the density of the thermally-induced spin-flips is small. In the disordered phase (above T_c), one can neglect the correlations between the positions of spin-flips in different chains and the density of the spin-flips (kinks and antikinks) is given by the Boltzmann formula: $n_s = e^{-\beta I}$. In the ordered phase, the interchain interactions bind kinks and antikinks within one chain into pairs, which is clear from the fact that $n_s \propto e^{-2\beta I}$ below T_c. As follows from Eq. (4.5) the binding energy V of such a pair is proportional to the distance R between kink and antikink:

$$V(R) = \tilde{I}_\perp R \,, \tag{4.71}$$

as over this distance the spin sign is opposite to $\langle\langle \sigma \rangle\rangle$. Thus, below $T_c(0)$, the density of the thermally induced kink-antikink pairs is:

$$n_{pair} \sim \bar{R}(T)\, e^{-2\beta I} \,, \tag{4.72}$$

where the factor $\bar{R}(T) = T/\tilde{I}_\perp$ is the average size of the pair at temperature T and comes from the sum over all possible distances between kinks and antikinks in the partition function. The density of spin-flips in the ordered phase equals $2n_{pair}$, in accordance with Eq. (4.54).

The transition between the ordered and disordered phases occurs when the kink-antikink pairs dissociate into free kinks and antikinks. Thus, at the critical temperature the average length of the kink-antikink pair is of the order of the average distance $1/n_s$ between spin-flips,

$$\bar{R}(T_c(0)) \sim \exp\left(\frac{I}{T_c(0)}\right), \tag{4.73}$$

which explains the physical content of Eq. (4.49) [22].

Next we discuss the density of spin-flips in the disordered phase induced predominantly by the random magnetic field [see Eq. (4.68)]. This equation coincides with the simple Imry and Ma estimate Eq. (4.2), except that the kink creation energy, I, is replaced by $I(T,\epsilon)$ defined in Eq. (4.58). This can be understood as follows: The spin-flips enter into the partition function with the weight: $w(T) = l(T)e^{-\beta I}$, where $l(T) \sim T^2/\epsilon$ is the thermal fluctuation of the spin-flip position in the presence of the random magnetic field. We can now write the weight in the form: $w(T) = e^{-\beta I(T,\epsilon)}$, where $I(T,\epsilon) = I - T\ln l(T)$ is the spin-flip free energy, which also includes the entropy of the spin-flip location. It is clear that the free energy, rather than the "bare" kink creation energy, I, should enter into the correct expression Eq. (4.68) for the density of spin-flips.

Finally, we discuss the critical strength of the random magnetic field, given by Eq. (4.65), above which the system is disordered at all temperatures. In an isolated chain, spin-flips are induced by an arbitrarily weak random magnetic field [see Eq. (4.68)], because the distances between the spin-flips can be made as large as is necessary to compensate for the spin-flip creation energy by the energy of the interaction with the random magnetic field. In the presence of interchain interactions, however, the distances between spin-flips are not allowed to be arbitrarily large, because of the potential Eq. (4.71). The potential grows linearly with the distance R between kink and antikink, while the energy gain due to kink-antikink pair creation grows proportional to $\sqrt{R}$. Thus, in the presence of interchain interactions, the equation describing the balance between the energy gain and energy loss due to the creation of a kink-antikink pair of size R [cf. Eq. (4.1)],

$$2I + \tilde{I}_\perp R \sim 2\sqrt{\epsilon R}, \tag{4.74}$$

only has a solution if $\epsilon > \epsilon_c \sim \tilde{I}_\perp I$, in accordance with Eq. (4.65). For $\epsilon < \epsilon_c$ the distances between disorder-induced spin-flips in isolated chains are very large, so that they are suppressed by the interchain interactions and the system at zero temperature is in the ordered state. If, on the other hand, $\epsilon > \epsilon_c$ the system is disordered at all temperatures.

The dependence of the critical temperature on the disorder strength in the RFIM can be compared with that in another Ising-type model of disordered (spin-) Peierls systems considered in Ref. [22]. There it was assumed that impurities randomly cut the chains into finite segments, some of which, *e.g.*, the ones with an odd number of units, contain at least one soliton. This was modeled by an ensemble of finite Ising chains whose length are taken from a Poisson distribution and which are subjected to a mean field and four different kinds of boundary conditions. For small impurity concentration x, the critical temperature in that model decreases linearly with x, just as in the RFIM [see Eq. (4.52)]. On the other hand, for large x, $T_c(x) \propto 1/x$ and at zero temperature the ground state is ordered for all values of x. The absence of a critical concentration, above which LRO is destroyed, is related to the fact that in that model the

positions of spin-flips (solitons) within the finite chains are not fixed. At $T = 0$ the spin-flips are located near one of the chain ends to minimize the size of "wrong" domains. In the RFIM, however, the distances between neighboring spin-flips are governed by the energy balance Eq. (4.74) and cannot be made arbitrarily small, which results in the existence of a critical random-field strength.

4.6 Summary and conclusions

In this chapter, we studied the anisotropic RFIM, consisting of spin chains with interchain exchange interactions that are much weaker than the intrachain interactions. Treating the interchain interactions in the mean-field approximation, we found an analytical solution Eq. (4.43) for the free energy. The crux of our approach lies in the fact that in this chain mean-field approximation the free energy of the continuum version of the model can be related to a one-dimensional Brownian motion. We found the stationary solution of the corresponding Fokker-Planck equation, which enabled us to perform the average of the free energy over the random magnetic field realizations. From this, we obtained the order parameter as a function of temperature and random-field strength and, more specifically, the critical temperature below which LRO occurs as a function of the random-field strength. We also calculated the density of spin-flips in the chains. As we decribed in Section 4.5, our results have a clear physical interpretation.

The chain mean-field approximation restricts the validity of our results to $d > 2$, where thermodynamic quantities suffer much less from fluctuations than in lower dimensional systems. We believe that the critical temperature $T_c(\epsilon)$ given by Eq. (4.64) describes the phase transition in three dimensions qualitatively correct and is quantitatively correct for a strongly anisotropic realization of the RFIM. Clearly, our mean-field treatment of interchain interactions is not applicable in two dimensions, where LRO is lacking for all temperatures and (or) random-field strengths [11].

The one-dimensional RFIM had been introduced in the context of disorder-induced solitons in a single chain of the polymer *trans*-polyacetylene (Chapter 3). The present treatment of the anisotropic d-dimensional RFIM allows us to extend that study to include the soliton-antisoliton confinement that is imposed by electron hopping between neighboring polyacetylene chains in the bulk material. In particular, the exponential suppression of the density of spin-flips well below the critical random-field strength (see Eq. (4.70)) may be relevant to explain the absence of experimental signatures of these solitons. In the next chapter, we will focus more particularly on this application of the anisotropic RFIM and discuss the magnetic susceptibility of *trans*-polyacetylene.

Bibliography

[1] T. Nattermann, in *Spin Glasses and Random Fields*, ed. P. Young (World Scientific, Singapore), cond-mat/9705295.

[2] D.P. Belanger, in *Spin Glasses and Random Fields*, ed. P. Young (World Scientific, Singapore), cond-mat/9706042.

[3] S. Fishman and A. Aharony, J. Phys. C **12**, L729 (1979).

[4] J.P. Hill, Q. Feng, Q.J. Harris, R.J. Birgeneau, A.P. Ramirez, and A. Cassanho, Phys. Rev. B **55**, 356 (1997).

[5] Q. Feng, Q.J. Harris, R.J. Birgeneau, and J.P. Hill, Phys. Rev. B **55**, 370 (1997).

[6] T.R. Kirkpatrick and D. Belitz, Phys. Rev. Lett. **74**, 1178 (1996).

[7] A.M. Gutin, V.I. Abkevich, and E.I. Shakhnovich, Phys. Rev. Lett. **77**, 5433 (1996).

[8] J.V. Selinger and R.L.B. Selinger, Phys. Rev. Lett. **76**, 58 (1996).

[9] Y. Imry and S. Ma, Phys. Rev. Lett. **35**, 1399 (1975).

[10] Y. Imry, J. Stat. Phys. **34**, 849 (1984).

[11] J. Imbrie, Phys. Rev. Lett. **53**, 1747 (1984); J. Imbrie, Commun. Math. Phys. **98**, 145 (1985); J. Imbrie, Physica A **140**, 291 (1986).

[12] A.J. Heeger, S. Kivelson, J.R. Schrieffer, and W.P. Su, Rev. Mod. Phys. **60**, 781 (1988).

[13] G. Paladin and M. Serva, Phys. Rev. Lett. **69**, 706 (1992).

[14] Y. Imry, P. Pincus, and D. Scalapino, Phys. Rev. B **12** 1978 (1975).

[15] E. Fradkin and L. Susskind, Phys. Rev. D **17**, 2637 (1978).

[16] J.B. Kogut, Rev. Mod. Phys. **51**, 659 (1979).

[17] N.G. van Kampen, *Stochastic Processes in Physics and Chemistry* (North-Holland Publishing, 1981).

[18] R. Kubo, M. Toda, and N. Hashitsume, *Statistical Physics II* (Springer, Berlin, 1995).

[19] *see e.g.* M. Abramowitz and I.A. Stegun, *Handbook of Mathematical Functions* (Dover Publications, New York, 1972).

[20] L. Onsager, Phys. Rev. **64**, 117 (1944).

[21] *see e.g.* R.J. Baxter, *Exactly Solved Models in Statistical Mechanics* (Academic Press, London, 1982) *or* Ashok Das, *Field Theory* (World Scientific, Singapore, 1993).

[22] D. Khomskii, W. Geertsma, and M. Mostovoy, Czech. Journ. of Phys. **46**, Suppl. S6, 3229 (1996); M. Mostovoy and D. Khomskii, Z. Physik B **103**, 209 (1997).